

# Canonical Transient Receptor Potential 6 (TRPC6), a Redox-regulated Cation Channel<sup>\*[5]</sup>

Received for publication, December 9, 2009, and in revised form, May 21, 2010 Published, JBC Papers in Press, May 25, 2010, DOI 10.1074/jbc.M109.093500

Sarabeth Graham<sup>#1</sup>, Min Ding<sup>#1</sup>, Yanfeng Ding<sup>‡</sup>, Sherry Sours-Brothers<sup>#2</sup>, Rafal Luchowski<sup>§</sup>, Zygmunt Gryczynski<sup>§</sup>, Thomas Yorio<sup>¶</sup>, Haiying Ma<sup>¶</sup>, and Rong Ma<sup>#3</sup>

From the <sup>‡</sup>Department of Integrative Physiology and Cardiovascular Research Institute, <sup>§</sup>Department of Molecular Biology and Immunology, and <sup>¶</sup>Department of Pharmacology and Neuroscience, University of North Texas Health Science Center, Fort Worth, Texas 76107

This study examined the effect of H<sub>2</sub>O<sub>2</sub> on the TRPC6 channel and its underlying mechanisms using a TRPC6 heterologous expression system. In TRPC6-expressing HEK293T cells, H<sub>2</sub>O<sub>2</sub> significantly stimulated Ca<sup>2+</sup> entry in a dose-dependent manner. Electrophysiological experiments showed that H<sub>2</sub>O<sub>2</sub> significantly increased TRPC6 channel open probability and whole-cell currents. H<sub>2</sub>O<sub>2</sub> also evoked a robust inward current in A7r5 vascular smooth muscle cells, which was nearly abolished by knockdown of TRPC6 using a small interfering RNA. Catalase substantially attenuated arginine vasopressin (AVP)-induced Ca<sup>2+</sup> entry in cells co-transfected with TRPC6 and AVP V1 receptor. *N*-Ethylmaleimide and thimerosal were able to simulate the H<sub>2</sub>O<sub>2</sub> response. Dithiothreitol or glutathione-reduced ethyl ester significantly antagonized the response. Furthermore, both *N*-ethylmaleimide- and H<sub>2</sub>O<sub>2</sub>-induced TRPC6 activations were only observed in the cell-attached patches but not in the inside-out patches. Moreover, 1-oleoyl-2-acetyl-*sn*-glycerol effect on TRPC6 was significantly greater in the presence of H<sub>2</sub>O<sub>2</sub>. Biotinylation assays revealed a significant increase in cell surface TRPC6 in response to H<sub>2</sub>O<sub>2</sub>. Similarly, in cells transfected with TRPC6-EGFP, confocal microscopy showed a significant increase in fluorescence intensity in the region of the cell membrane and adjacent to the membrane. AVP also increased the fluorescence intensity on the surface of the cells co-transfected with TRPC6-EGFP and V1 receptor, and this response was inhibited by catalase. These data indicate that H<sub>2</sub>O<sub>2</sub> activates TRPC6 channels via modification of thiol groups of intracellular proteins. This cysteine oxidation-dependent pathway not only stimulates the TRPC6 channel by itself but also sensitizes the channels to diacylglycerol and promotes TRPC6 trafficking to the cell surface.

Accumulating evidence demonstrates that reactive oxygen species (ROS)<sup>4</sup> are not only the major contributors to a variety of diseases but also act as intracellular second messengers in several cellular signal transduction pathways (1–5). Hydrogen peroxide (H<sub>2</sub>O<sub>2</sub>), a ROS, is produced in response to receptor stimulation, which affects the function of various proteins, including ion channels, through oxidation of cysteine residues (6, 7). Specific inhibition of H<sub>2</sub>O<sub>2</sub> production nearly abolishes the responses induced by platelet-derived growth factor, epidermal growth factor, and angiotensin II (8–11). However, the molecular mechanism by which H<sub>2</sub>O<sub>2</sub> regulates cell function as an intracellular messenger has not been well described.

Canonical transient receptor potential (TRPC) channels are calcium-permeable cation channels involved in the regulation of intracellular calcium signaling. The TRPC channels comprise a family containing seven different members, designated TRPC1–7 (12–14). Physiologically, TRPC channel activation is triggered by activation of the phospholipase C pathway following activation of G-protein-coupled receptors or receptor tyrosine kinases (12). One downstream mechanism for TRPC channel activation in this signaling pathway is the stimulation of TRPC protein trafficking to the plasma membrane (15). TRPC6 protein expression and function have been described in the central nervous system, kidneys, and cardiovascular system (16–22). A link between altered expression level or function of TRPC6 channel and cardiovascular and renal diseases has also been established in recent studies (19, 23–25). Although the physiological and pathophysiological relevance of TRPC6 channel is evident, the regulatory mechanism for the channel function is currently unclear at the molecular level. Recent studies have called attention to the modulation of TRP channels by the cellular redox (6, 26, 27), which may underlie a novel mechanism for agonist-initiated cellular responses.

This study was performed to investigate whether ROS activated the TRPC6 channel and, furthermore, what the underlying mechanisms were for the ROS effect. Our findings suggest that H<sub>2</sub>O<sub>2</sub> activated TRPC6 channels through modification of protein thiol groups in intracellular mediators, through

\* This work was supported, in whole or in part, by National Institutes of Health Grant 1 RO1 DK079968-01A2 from NIDDK (to R. M.). This work was also supported by American Diabetes Association Grant 7-07-RA-99 (to R. M.), American Heart Association Grant 09GRNT2260926 (to R. M.), and a National Science Foundation SCORE Fellowship from the Graduate School of Biomedical Science, University of North Texas Health Science Center (to S. G.).

<sup>#</sup> Author's Choice—Final version full access.

[5] The on-line version of this article (available at <http://www.jbc.org>) contains supplemental Figs. S1 and S2 and Table S1.

<sup>1</sup> Both authors contributed equally to this work.

<sup>2</sup> Present address: Dept. of Internal Medicine, Division of Nephrology, University of Texas Southwestern Medical Center, Dallas, TX 75300. Tel.: 214-648-5602; E-mail: sherry.sours-brothers@utsouthwestern.edu.

<sup>3</sup> To whom correspondence should be addressed: RES-302G, 3500 Camp Bowie Blvd., Dept. of Integrative Physiology, University of North Texas Health Science Center, Fort Worth, TX 76107. Tel.: 817-735-2516; Fax: 817-735-5084; E-mail: rma@hsc.unt.edu.

<sup>4</sup> The abbreviations used are: ROS, reactive oxygen species; DTT, dithiothreitol; NEM, *N*-ethylmaleimide; OAG, 1-oleoyl-2-acetyl-*sn*-glycerol; GFP, green fluorescent protein; EGFP, enhanced GFP; siRNA, small interfering RNA; RNAi, RNA interference; GSH-MEE, glutathione reduced ethyl ester; AVP, arginine vasopressin; TRPC, transient receptor potential channel; pF, picrofarad; DAG, diacylglycerol.

enhancement of the sensitivity of the channels to diacylglycerol (DAG), and through promotion of TRPC6 protein trafficking to the cell membrane.

## EXPERIMENTAL PROCEDURES

**Cell Culture and Transient Transfection**—Both human embryonic kidney 293 (HEK293T) cells and A7r5 vascular smooth muscle cells were purchased from ATCC (Manassas, VA) and were cultured in Dulbecco's modified Eagle's medium (Hyclone SH30021.01 for HEK293T and ATCC 30–2002 for A7r5) with 25 mM HEPES, containing 10% fetal bovine serum and 100 units/ml penicillin/streptomycin. HEK293T cells were subcultured to no more than 50 generations, and A7r5 cells were used from passage 8 to 10. Cells were cultured in an incubator in 5% CO<sub>2</sub> at 37 °C. For HEK293 cells, all plasmids were transiently transfected using GenJet (SigmaGen, Gaithersburg, MD) following the protocols provided by the manufacturer. To identify the positively transfected cells in patch clamp experiments, a GFP expression plasmid was co-transfected with other constructs at a ratio of 1:9 (GFP/other construct). For TRPC6 knockdown studies in A7r5 cells, we transfected the cells with a sense sequence of rat TRPC6 siRNA (GGAAUAUGCUUGACUUUGGAAUGUU) or with a scrambled sequence (nontargeting siRNA 1, Dharmacon D-001810-01-20) using DharmaFECT 2 (Dharmacon Inc., Lafayette, CO) following the manufacturer's protocol. Briefly, A7r5 cells were plated in antibiotic-free medium in 35-mm dishes 12 h prior to transfection. For transfection, 4 μl of 50 μM TRPC6 siRNA sequence or scrambled sequence and 4 μl of DharmaFECT transfection reagent were added to 200 μl of serum-free Dulbecco's modified Eagle's medium, respectively, in two tubes. After 5 min of incubation, the two tubes were mixed and incubated for another 20 min. The DharmaFECT2/oligonucleotide mixture was then diluted with serum-free Dulbecco's modified Eagle's medium (1:4) and was added to A7r5 cells in a final concentration of 0.1 μM. The cells were incubated for 24–48 h on coverslips before electrophysiology measurements were undertaken.

**Generation of Rat *Trpc6* RNA Interference Construct**—A 53-nucleotide hairpin oligonucleotide that contained a sequence specifically targeting rat *Trpc6* mRNA was designed using siRNA Designer tool (Promega). The sequences used in the present study were as follows: forward (5'–3') TCTCGAACGGCCTCATGATTATTAAGTTCTCTAATAATCATGAGGCCGTTCT (boldface characters indicate target sequence) and reverse (5'–3') CTGCAGGAACGGCCTCATGATTATTAGAGAACTTAATAATCATGAGGCCGTTCT. To avoid possible nonspecific gene silencing, the designed sequence was blasted at [www.ncbi.nlm.nih.gov/BLAST](http://www.ncbi.nlm.nih.gov/BLAST) to compare with the rat genome data base. A scrambled sequence was used as a negative control for RNA interference. The two complementary oligonucleotides were synthesized (by IDT), annealed, and ligated into the linearized pGeneClip<sup>TM</sup> hMGFP vector (Promega). All procedures were performed as directed by the manufacturer's instruction.

**Generation of TRPC6-EGFP Expression Construct**—For cell imaging studies, rat wild-type *Trpc6* gene was subcloned into the mammalian expression vector pEGFP-N1(Clontech) to obtain a fusion fluorescence protein. The rat *Trpc6* gene was

amplified by high fidelity PCR, with an rTRPC6 expression plasmid as the template. The upstream primer 5'-GGG GGC TAG CCA CCA TGA GCC AGA GCC CGG GG-3' contains a Kozak sequence. The downstream primer 5'-GGG GTA CCG TTC TGC GGC TTT CCT CTT GTT T-3' eliminated the stop codon and restored the EGFP reading frame. The amplified product (insert) was digested with NheI and KpnI. The vector pEGFP-N1 was treated with calf intestinal phosphatase followed by the digestion with NheI and KpnI. The purified insert and vector were ligated to obtain the fusion TRPC6-EGFP sequence, which was verified by sequencing (SeqWright, Houston, TX).

**Patch Clamp Procedure**—Conventional cell-attached and whole-cell voltage clamp configurations were employed as described in our previous studies (28–31). Inside-out patch clamp was also utilized. Channel currents were measured with a Warner PC-505B amplifier (Warner Instrument Corp., Hamden, CT) and pClamp 9.2 (Axon Instrument, Foster City, CA). The compositions of extracellular and pipette solutions for different modes of patch clamp were provided in [supplemental Table S1](#). The resistances of the glass pipettes (plain; Fisher) were 5–6 megohms for whole-cell patch clamp and 8–10 megohms for the cell-attached and inside-out patch clamps. A gap-free protocol was used for all modes of patch clamp experiments. In all experiments utilizing transfected cells, only GFP-labeled cells were targeted for patching. In the whole-cell patch clamp experiments, after the whole-cell configuration was achieved, cell capacitance and series resistance were compensated prior to recording. The whole-cell currents were continuously measured at a holding potential of –60 mV. Channel traces were filtered at 1 kHz for the whole-cell patch recording and 10 kHz for the cell-attached and inside-out patch recordings. To exclude the influence of fluid flow on channel activity upon delivery of chemicals, the bathing solution continuously flowed throughout the experiments. The flow rate was adjusted by gravity and controlled by a multiple channel perfusion system (ValveLink<sup>TM</sup>8, Automate Scientific, Inc.). The whole-cell currents were normalized to the cell capacitance and expressed as current density (pA/pF). Single channel activity was calculated as channel open probability ( $NP_o$ ). Clampfit 9.2 software (Axon Instrument, Foster City, CA) was used to analyze channel currents.

**Fluorescence Measurement of  $[Ca^{2+}]_i$** —Intracellular Ca<sup>2+</sup> concentration ( $[Ca^{2+}]_i$ ) was assessed by measuring fura-2 fluorescence using dual excitation wavelengths as described previously (28, 29, 32). HEK293T cells, grown on a coverslip (22 × 22 mm), were loaded with fura-2 by incubation for ~50 min at room temperature in the dark in physiological saline solution containing 2 μM acetoxymethyl ester of fura-2 (fura-2/AM) and 0.018 g/dl pluronic F-127 (Molecular Probes, Eugene, OR). This was followed by washing three times with physiological saline solution. The cells were then incubated with fura-2-free physiological saline solution for an additional ~20 min. The coverslip was then placed in a perfusion chamber (Warner, model RC-2OH) mounted on the stage of a Nikon Diaphot inverted microscope. Fura-2 fluorescence was monitored by ratiometry (excitation at 340 and 380 nm, emission at 510 nm) using Metafluor software (Universal Imaging, West Chester, PA) at

## Regulation of TRPC6 by Reactive Oxygen Species

room temperature. In Fig. 4,  $[Ca^{2+}]_i$  was calculated using the formula described by Grynkiewicz *et al.* (33). Calibrations were performed *in vivo* at the end of each experiment, and conditions of high  $[Ca^{2+}]_i$  were achieved by addition of 5  $\mu M$  ionomycin, whereas conditions of low  $[Ca^{2+}]_i$  were obtained by addition of 5 mM EGTA.

**Biotinylation Assay**—Monolayer cells (~80% confluent in a 10-cm plate) were washed three times with cold phosphate-buffered saline. The cells were then incubated with 1.5 mg/ml of sulfo-NHS-SS-biotin (Pierce) for 30 min at 4 °C with shaking. Biotinylation was terminated by washing cells three times with cold phosphate-buffered saline containing 10 mM glycine. Cells were then incubated with 1 ml of cold lysis buffer (containing proteinase inhibitors) for 1 h at 4 °C with shaking. Cells were then scraped, and lysates were collected into a 1.5-ml Eppendorf tube. The cell lysates were rocked for 20 min at 4 °C and then centrifuged at  $21,000 \times g$  for 15 min at 4 °C. 100  $\mu l$  of lysates were saved for immunoblotting as inputs. The rest of the supernatants were mixed with 100  $\mu l$  of lysis buffer (total volume: 1 ml) and then incubated with 50  $\mu l$  of a slurry of immobilized streptavidin beads (Pierce) overnight while shaking. The beads were spun down and washed three times with lysis buffer. The biotinylated samples were then analyzed by Western blot.

**Western Blot**—Western blot was performed as described in our previous publications (21, 28, 29). In brief, HEK293T cell lysates were fractionated by 10% SDS-PAGE, transferred to polyvinylidene difluoride membranes, and probed with primary TRPC6 or  $\beta$ -actin antibodies. Bound antibodies were visualized with Super Signal West Femto or Pico Luminol/Enhancer Solution (Pierce).

**TRPC6 Trafficking Assay in Live Cells Using Confocal Microscopy**—HEK293 cells were grown on  $20 \times 20$ -mm nonfluorescence coverslips (Menzel-Glaser 1, Germany) until ~60% confluence and were transfected with either TRPC6-EGFP or EGFP expression plasmids. The cells were used for the trafficking assay about 24 h after transfection. The cells were washed three times with physiological saline solution and then mounted to an adapter on an Olympus IX71 inverted microscope stage. All fluorescence imaging experiments were performed on a MicroTime200 time-resolved confocal microscope (PicoQuant GmbH) equipped with an Olympus UPlanSApo (60 $\times$  magnification, NA = 1.2, water immersion) objective at room temperature. The fluorescence light was collected through the objective onto the avalanche photo-diode (Mico Photon Device PD1CTC) and processed by the PicoHarp300 time-correlated single-photon counting module. Cell images were captured before application, immediately, 2, and 4 min after application of  $H_2O_2$ . The excitation wavelength was 470 nm, and fluorescence emission was observed through 500-nm-long wavelength pass filter. The control nontransfected cells show a negligible emission intensity signal. The fluorescence intensity in the region of the plasma membrane was quantitatively analyzed offline using a software SymPhoTime (version 5.0) package, which controlled the data acquisition as well.

**Materials**—The rat *Trpc6* expression plasmids (pEF-BOS-SK-TRPC6A) were obtained from Dr. David Saffen at the Ohio State University. GFP vectors were obtained from Dr. Leonidas

Tsiokas (University of Oklahoma Health Sciences Center, Oklahoma City). Human arginine vasopressin receptor 1A (V1R) expression plasmid was purchased from University of Missouri-Rolla, cDNA Resource Center (Rolla, MO). Antibodies and all chemicals were purchased from Sigma.

**Statistical Analysis**—Data were reported as means  $\pm$  S.E. One-way analysis of variance, one-way repeated measures analysis of variance plus Student-Newman-Keuls test, Student's unpaired *t* test, and Student's paired *t* test were used to analyze the differences among multiple groups or multiple treatments in the same group, between two groups, and before and after treatment in the same group, respectively.  $p < 0.05$  was considered statistically significant. Statistical analysis was performed using SigmaStat (Jandel Scientific, San Rafael, CA).

## RESULTS

**TRPC6 Channel-mediated Responses in a Heterologous Expression System**—TRPC6 is a  $Ca^{2+}$ -permeable cation channel that has been shown to have a physiological role in a variety of cell types (19). One feature of the channel is to be selectively and directly activated by DAG or its membrane-permeable analog, 1-oleoyl-2-acetyl-*sn*-glycerol (OAG) (34, 35). To study the TRPC6 channels, we overexpressed TRPC6 in HEK293T cells by transient transfection of the pEF-BOS-SK-TRPC6A construct, which significantly increased the TRPC6 protein expression level (Fig. 1A). Consistent with previous publications (36–38), two bands corresponding to TRPC6 protein were detected, one at ~100 kDa and the other at ~120 kDa. The lower molecular weight band might represent newly synthesized TRPC6 protein, whereas the higher molecular weight band might represent a glycosylated version of TRPC6 that has been reported by Dietrich *et al.* (39). The  $Ca^{2+}$  imaging and patch clamp experiments were then performed to examine whether these exogenous TRPC6 channels were functional. Fura-2 fluorescence measurement showed that OAG-stimulated  $Ca^{2+}$  entry was significantly increased in TRPC6-expressing cells when compared with untransfected or mock-transfected cells (Fig. 1B). OAG has been known to activate the TRPC6 channel directly, *i.e.* independent of activation of protein kinase C (34, 35). In agreement with this mechanism, inhibition of protein kinase C with calphostin C (1  $\mu M$ ) did not affect the OAG-induced  $Ca^{2+}$  response in TRPC6-expressing cells (Fig. 1B). Furthermore,  $La^{3+}$  (2  $\mu M$ ), a potent TRPC channel blocker, completely abolished the OAG-induced  $Ca^{2+}$  entry in the cells expressing TRPC6. In cell-attached patch clamp experiments, overexpression of TRPC6 significantly raised the single channel  $NP_o$  in the resting state (Fig. 1C). OAG treatment dramatically increased channel activity in the cells expressing TRPC6 but had no significant effect on the untransfected or mock-transfected cells. The OAG response in the TRPC6-expressing cells was nearly abolished by knocking down *Trpc6* with RNAi (Fig. 1C), which substantially reduced the TRPC6 protein expression (Fig. 1A). Taken together, the data from the  $Ca^{2+}$  imaging and patch clamp experiments strongly suggest that the exogenous TRPC6 channels expressed in HEK293T cells were fully functional. Therefore, this heterologous expression system was used as a cell model for studying the regulation of TRPC6 channel function by  $H_2O_2$  in this study.

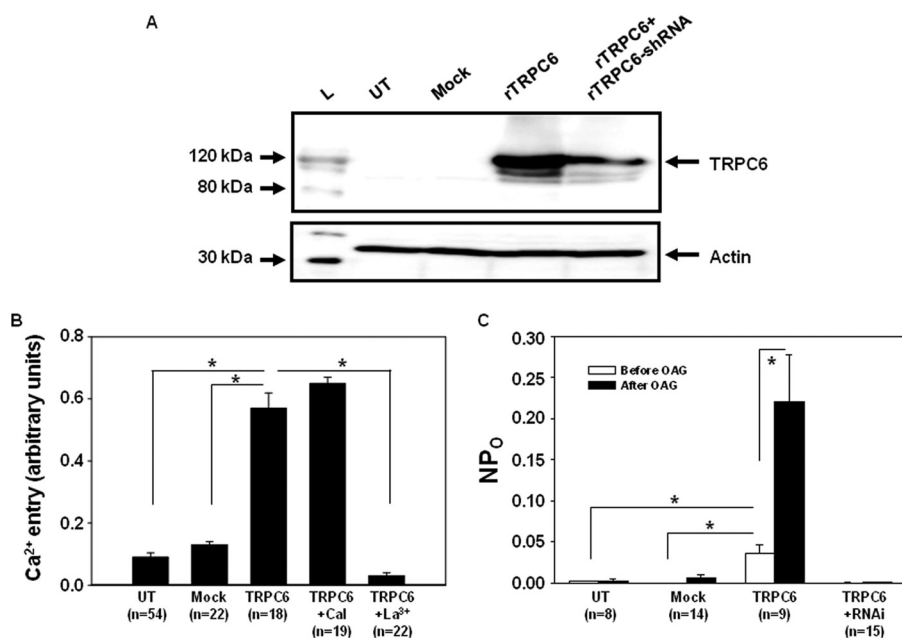


**FIGURE 1. TRPC6 channel response in TRPC6-expressing HEK293T cells.** *A*, Western blot, showing the expression level of TRPC6 protein in untransfected (UT) HEK293T cells and the HEK293T cells with transient transfection of vector (*Mock*), rat TRPC6 expression plasmid (*rTRPC6*), and *rTRPC6* plus RNAi constructs for rat TRPC6 (*rTRPC6+shRNA*). TRPC6 was probed with rabbit anti-TRPC6 antibody. *L*, ladder of a protein marker. Actin was used as a loading control. *B*, fura-2 fluorescence measurement of Ca<sup>2+</sup> entry response stimulated by 100  $\mu$ M OAG in untransfected (UT), vector-transfected (*Mock*), and TRPC6-expressing (*TRPC6*) cells, and TRPC6-expressing cells treated with 1  $\mu$ M calphostin C (*TRPC6+Cal*) or 2  $\mu$ M La<sup>3+</sup> (*TRPC6+La<sup>3+</sup>*). *C*, cell-attached patch clamp, showing channel open probability (NP<sub>0</sub>) in response to 100  $\mu$ M OAG in untransfected (UT), vector-transfected (*Mock*), TRPC6 expression plasmid (*TRPC6*)-transfected, and TRPC6 expression plasmid plus its RNAi construct-transfected (*TRPC6+RNAi*) HEK293T cells. *B* and *C*, \*,  $p < 0.05$ , between the groups as indicated. *n* indicates the number of cells analyzed from at least six different transfections.

**Stimulation of Ca<sup>2+</sup> Entry by H<sub>2</sub>O<sub>2</sub> in TRPC6-expressing Cells**—By using the established heterologous TRPC6 expression system, we performed Ca<sup>2+</sup>-imaging experiments to evaluate if there was any effect of H<sub>2</sub>O<sub>2</sub> on TRPC6 channel activity. As shown in Fig. 2*A*, in a Ca<sup>2+</sup>-free extracellular solution, application of H<sub>2</sub>O<sub>2</sub> from 0.01 to 100  $\mu$ M did not change the cytosolic Ca<sup>2+</sup> level, suggesting that these concentrations of H<sub>2</sub>O<sub>2</sub> did not affect Ca<sup>2+</sup> release. However, after an ~3-min treatment with H<sub>2</sub>O<sub>2</sub>, Ca<sup>2+</sup> readmission resulted in an elevation of [Ca<sup>2+</sup>]<sub>i</sub>, the peak of which occurred ~2 min after Ca<sup>2+</sup> addition. This Ca<sup>2+</sup> entry response was dose-dependent with a maximum response at nearly 10  $\mu$ M (Fig. 2*C*). Thus, we used this concentration of H<sub>2</sub>O<sub>2</sub> for all the remaining experiments. However, in the empty vector-transfected (*Mock*) cells, the stimulatory effect of H<sub>2</sub>O<sub>2</sub> on the Ca<sup>2+</sup> entry was significantly lower, and no dose-dependent effect of H<sub>2</sub>O<sub>2</sub> was observed (Fig. 2, *B–D*). The slight increase in [Ca<sup>2+</sup>]<sub>i</sub> upon Ca<sup>2+</sup> readmission in the *Mock* control cells might result from the endogenous TRPC6 or other TRPCs.

**Stimulation of Membrane Currents by H<sub>2</sub>O<sub>2</sub> in TRPC6-expressing Cells**—To further determine the H<sub>2</sub>O<sub>2</sub> effect on TRPC6 channels, we carried out whole-cell patch clamp experiments in TRPC6-expressing and mock-control (GFP-transfected) cells. As shown in Fig. 3*A*, application of 10  $\mu$ M H<sub>2</sub>O<sub>2</sub> induced a robust inward current in the TRPC6-transfected cells, but only a weak response in the control cells. The current response reached its peak about 2 min after H<sub>2</sub>O<sub>2</sub> application and then was maintained at a steady but increased

level for at least 5 min. Removal of H<sub>2</sub>O<sub>2</sub> significantly reversed the response. The small increase in the inward current by H<sub>2</sub>O<sub>2</sub> in the *Mock* cells may be attributed to the endogenous channels present in HEK293T cells. Summary data (Fig. 3*B*) from 10 TRPC6-expressing cells and 9 control cells showed that the H<sub>2</sub>O<sub>2</sub>-induced response was significantly greater in TRPC6-transfected cells ( $-101 \pm 28$  pA/pF *versus*  $-16 \pm 3$  pA/pF, TRPC6-transfected cells *versus* *Mock*-transfected cells,  $p < 0.05$ ).

In the cell-attached mode of patch clamp, we also found that H<sub>2</sub>O<sub>2</sub> significantly increased the single channel activity in TRPC6-transfected cells (Fig. 3, *C* and *D*). Consistent with the whole-cell mode of patch recordings, the channel response reached the maximal level about 2 min after H<sub>2</sub>O<sub>2</sub> application and was sustained in a significantly active state thereafter (Fig. 3*C*). For further quantification of our single channel data before and after application of H<sub>2</sub>O<sub>2</sub>, we calculated amplitude and open time dis-

tributions of single-channel currents shown in the representative traces (Fig. 3*C*). As revealed in Fig. 3*D* (*upper panels*), H<sub>2</sub>O<sub>2</sub> stimulation did not change the amplitude but increased the frequency of the currents. A calculation from eight recorded cells showed the unitary currents before and after H<sub>2</sub>O<sub>2</sub> treatment (Fig. 3*E*). However, in the presence of H<sub>2</sub>O<sub>2</sub>, the duration of the channel in the open state increased remarkably (4.1 *versus* 17.4 milliseconds, pre-H<sub>2</sub>O<sub>2</sub> *versus* post-H<sub>2</sub>O<sub>2</sub>, Fig. 3*D*, *lower panels*). These electrophysiological data are consistent with the Ca<sup>2+</sup>-imaging data and further suggest that the TRPC6 channel is activated by H<sub>2</sub>O<sub>2</sub>.

**Physiological Relevance of H<sub>2</sub>O<sub>2</sub>-induced TRPC6 Activation**—To determine whether endogenous H<sub>2</sub>O<sub>2</sub> generated from a physiological pathway could also activate TRPC6, we conducted an experiment in which the TRPC6-mediated Ca<sup>2+</sup> influx in response to arginine vasopressin (AVP) was examined in the presence and absence of catalase, a H<sub>2</sub>O<sub>2</sub>-decomposing enzyme. In HEK293T cells expressing TRPC6 alone, AVP (100 nM) did not evoke internal Ca<sup>2+</sup> release, and Ca<sup>2+</sup> readmission only resulted in a slight increase in [Ca<sup>2+</sup>]<sub>i</sub>. However, in the cells expressing both TRPC6 and V1R, AVP stimulation elicited an obvious Ca<sup>2+</sup> release, and importantly, addition of Ca<sup>2+</sup> back into the Ca<sup>2+</sup>-free bathing solution induced a robust rise in [Ca<sup>2+</sup>]<sub>i</sub>. This entry response was significantly attenuated in the cells pretreated with PEG-catalase (250 units/ml for 30 min) (Fig. 4, *A* and *B*). Ca<sup>2+</sup> release had a tendency to decrease (statistically insignificant) because of catalase treatment (Fig. 4*C*), so we normalized Ca<sup>2+</sup> entry to Ca<sup>2+</sup> release to exclude the

## Regulation of TRPC6 by Reactive Oxygen Species

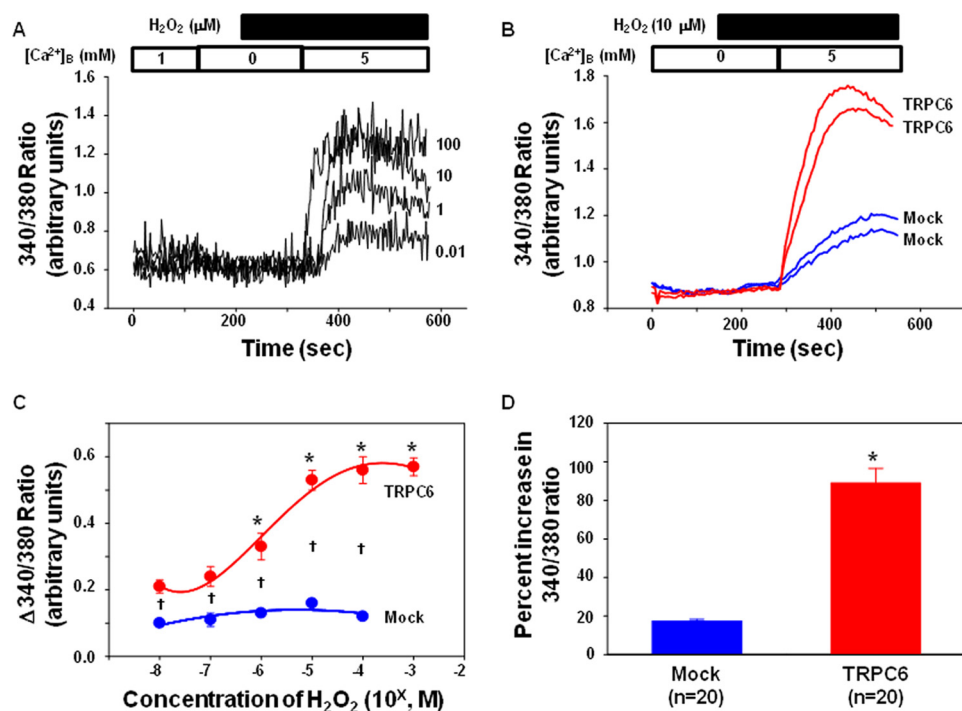


**FIGURE 2. Effect of  $H_2O_2$  on the intracellular  $Ca^{2+}$  signal in TRPC6-expressing and empty vector-transfected HEK293T cells.** *A*, representative traces, showing the changes in intracellular  $Ca^{2+}$  level upon 5 mM  $Ca^{2+}$  readdition to a  $Ca^{2+}$  free bathing solution in cells treated with different concentrations of  $H_2O_2$ . The  $Ca^{2+}$  concentration in the bathing solution is indicated by the numbers inside the top open bar. Application of  $H_2O_2$  is indicated by the top solid bar.  $[Ca^{2+}]_B$  indicates the  $Ca^{2+}$  concentration in the bathing solution. The numbers next to each trace indicate the concentration of  $H_2O_2$  ( $\mu M$ ) applied. *B*, representative traces, displaying intracellular  $Ca^{2+}$  response to  $Ca^{2+}$  readdition in vector-transfected (Mock) and rTRPC6-transfected (TRPC6) cells in the presence of 10  $\mu M$   $H_2O_2$ . The  $Ca^{2+}$  concentration in the bathing solution is indicated by the numbers inside the top open bar. Application of  $H_2O_2$  is indicated by the top solid bar.  $[Ca^{2+}]_B$  indicates the  $Ca^{2+}$  concentration in the bathing solution. *C*, summary data from five sets of TRPC6-transfected cells and two sets of empty vector-transfected cells, showing a dose-dependent response of  $Ca^{2+}$  entry on  $H_2O_2$  treatments in TRPC6-expressing but not in vector-transfected cells.  $\Delta 340/380$  ratio indicates the difference in the values before addition and the peak values after addition of 5 mM  $Ca^{2+}$  solution, representing the  $Ca^{2+}$  entry response. The numbers of cells in each group are from 16 to 25. \*,  $p < 0.05$ , compared with  $10^{-8}$  M in TRPC6-transfected cells; †,  $p < 0.05$ , comparison between TRPC6-transfected and Mock-transfected cells at corresponding doses. *D*, percent increases in the ratios of 340:380 in response to 10  $\mu M$   $H_2O_2$  in Mock- and TRPC6-transfected cells.  $n$  indicates the number of cells analyzed. \*,  $p < 0.05$ , TRPC6 versus Mock.

possibility that the attenuation of  $Ca^{2+}$  influx by catalase treatment was due to decreased depletion of internal  $Ca^{2+}$  stores. As shown in Fig. 4D, the normalized  $Ca^{2+}$  entry was also significantly inhibited by catalase. 2',7'-Dichlorofluorescein measurements verified that AVP stimulation produced significant amounts of  $H_2O_2$  in TRPC6 and V1R-co-expressing cells, and catalase treatment significantly decreased the AVP-induced elevation of intracellular  $H_2O_2$  (supplemental Fig. S1).

To further explore the physiological relevance of the redox-sensitive TRPC6, we carried out whole-cell patch clamp experiments to examine the effect of  $H_2O_2$  on the endogenous TRPC6 channels in A7r5 rat aortic smooth muscle cells. In this cell type, TRPC6 is the predominant TRPC isoform and the major channel contributing to the  $Ca^{2+}$  signal associated with the phospholipase C pathway (35). As shown in Fig. 4, E and G, application of 100  $\mu M$   $H_2O_2$  induced a significant inward current within  $\sim 2$  min in the cells transfected with a scrambled sequence of *Trpc6* (Scramble). However, this response was nearly abolished by knockdown of *Trpc6* with siRNA (siRNA-T6). An efficient suppression of TRPC6 protein expression by siRNA-T6 was verified by Western blot (Fig. 4F).

These results from both the  $Ca^{2+}$  imaging assay and electrophysiology studies in HEK293 cells and vascular smooth muscle cells, respectively, suggest that the activation of TRPC6 channel by  $H_2O_2$  is a physiological mechanism.

**Regulation of TRPC6 Channel by  $H_2O_2$  through Modification of Thiol Groups**—Cysteine residues are redox-sensitive and susceptible to thiol oxidation by  $H_2O_2$ . In an effort to deduce the mechanism for regulation of the TRPC6 channel by  $H_2O_2$ , we chose several different oxidizing and reducing agents specific for thiol groups for further experimentation. *N*-Ethylmaleimide (NEM) and thimerosal, cell-permeable thiol-oxidizing agents, and dithiothreitol (DTT) and glutathione-reduced ethyl ester (GSH-MEE), cell membrane permeable thiol-reducing agents, were used to evaluate their effects on TRPC6-mediated  $Ca^{2+}$  entry. As shown in Fig. 5A, both NEM (300  $\mu M$ ) and thimerosal (100  $\mu M$ ) significantly increased  $Ca^{2+}$  entry as compared with their vehicle controls in TRPC6-expressing cells. Reducing thiol groups with DTT (1 mM) or GSH-MEE (1 mM) dramatically and significantly inhibited the  $H_2O_2$ -stimulated  $Ca^{2+}$  entry in TRPC6-transfected cells (Fig. 5B). These results suggest that thiol modification

was involved in  $H_2O_2$ -induced TRPC6 activation.

**Cellular Localization of Thiol Groups Involved in TRPC6 Channel Activation**—Cell-attached and inside-out patch clamp experiments were carried out in TRPC6-expressing cells to determine whether the  $H_2O_2$  effect was via a direct action on cysteine residues in TRPC6 proteins or through an indirect pathway, *i.e.* by acting on cytosolic proteins that subsequently activated TRPC6 channel. In the cell-attached mode, application of NEM (300  $\mu M$ ) into the bathing solution significantly raised the  $NP_o$  of the channels (Fig. 6, A and B). In contrast to the stimulatory effect seen in the cell-attached patches (Fig. 3, C and D, and Fig. 7, A and B), neither  $H_2O_2$  nor NEM was able to evoke a discernible increase in channel activity during the entire period of observation ( $\sim 4$  min) when applied into the bath in the inside-out excised patches. However, subsequent delivery of OAG into the bathing solution dramatically and significantly activated the channels, suggesting that the channels did not lose their capability to be activated after excision (Fig. 6, C and D). These results suggested that cytosolic components were required for thiol oxidation-associated TRPC6 channel activation.

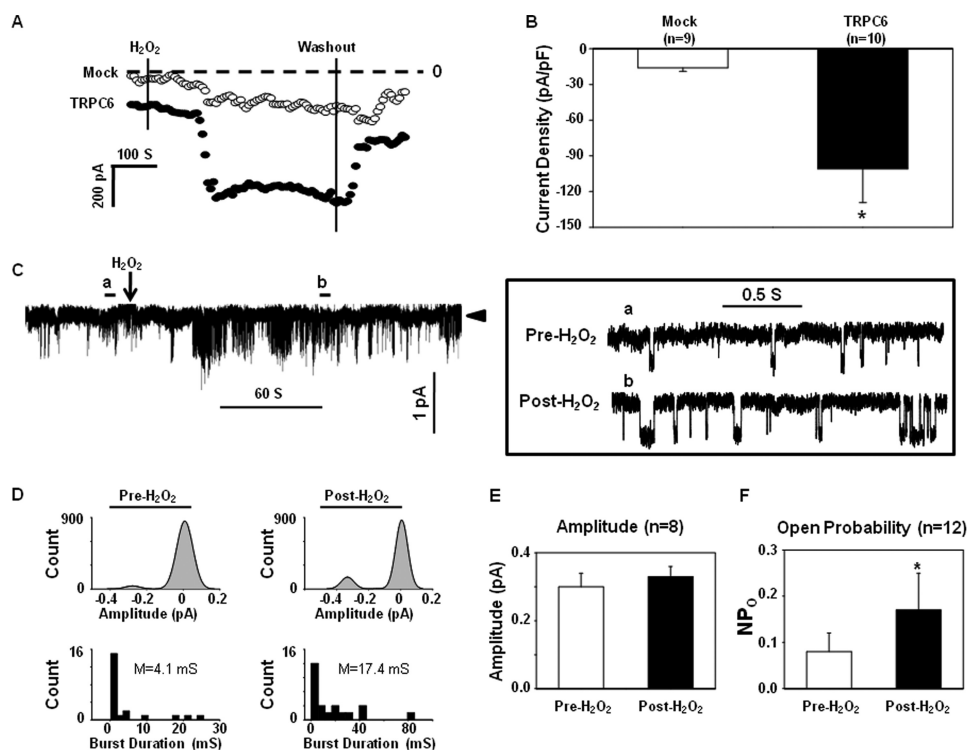


**FIGURE 3. Effect of  $H_2O_2$  on whole-cell currents (A and B, whole-cell patch) and single channel currents (C–F, cell-attached patch) in TRPC6-expressing HEK293T cells.** A, representative whole-cell current measurements obtained by a Gap-free protocol in a Mock (*open circles*)- and a TRPC6-transfected (*solid circles*) cell at a holding potential of  $-60$  mV. The *dashed lines* indicate zero currents. Application and removal of  $H_2O_2$  are indicated by the *vertical lines*. B, summary data, showing the  $H_2O_2$  effect on the whole-cell currents in the Mock control and TRPC6-expressing cells. The responses were measured by the difference between the membrane current before application of  $H_2O_2$  and the peak current after application of  $H_2O_2$ . The whole-cell currents are expressed as current density (pA/pF), normalized to the cell membrane capacitance. *n* indicates the number of cells analyzed. Asterisk indicates statistically significant difference compared with Mock (Student's *t* test). C, representative traces of single channel currents in a cell-attached patch. *Left panel*, a real time continuous recording. The *arrowhead* indicates the closed state of the channels. *Downward deflections* indicate inward currents. *Right panel*, the time-expanded portions of the selected regions in the upper trace, indicated by *a* (Pre- $H_2O_2$ ) and *b* (Post- $H_2O_2$ ). D, amplitude histograms (*upper panels*) and open time distributions (*bottom panels*) of the currents before (*left panels*) and after (*right panels*) application of  $H_2O_2$  in the traces shown in C. The amplitude histograms were fitted to Gaussian function. *M* in the *bottom panels* indicates mean open time. E, single channel amplitudes before and after application of  $10 \mu M H_2O_2$ . *n* indicates the number of cells analyzed. F, effect of  $H_2O_2$  on the  $NP_o$  of TRPC6 channels in 12 cells. \*,  $p < 0.05$ , compared with pre- $H_2O_2$  (paired Student's *t* test). The cells in each group of B, E, and F were from at least four sets of transfection.

**Sensitization of TRPC6 to DAG by  $H_2O_2$** —DAG generated from the phospholipase C signaling pathway is a physiological activator of the TRPC6 channel (34). Any mechanism that enhances the channel sensitivity to either endogenous or ligand-induced DAG is believed to increase the channel activity. To test if this mechanism was involved in the  $H_2O_2$  effect on TRPC6 channel, we performed cell-attached patch clamp experiments in TRPC6-expressing cells and compared the OAG-induced responses in the presence and absence of  $10 \mu M H_2O_2$ . As shown in Fig. 7A, a low concentration of OAG ( $0.1 \mu M$ ) did not significantly increase the channel activity in either case. Although the OAG-induced response ( $\Delta NP_o$ ) had a tendency to increase in the  $H_2O_2$ -treated cells, this increase did not reach a statistically significant level (Fig. 7B). However,  $100 \mu M$  OAG significantly increased the channel activity (Fig. 7C). Importantly, the OAG-induced channel activation was significantly enhanced (Fig. 7D) in the presence of  $H_2O_2$ . These data suggest that TRPC6 channel is more sensitive to OAG (DAG) in an oxidative environment.

**Stimulation of TRPC6 Protein Trafficking to the Cell Surface by  $H_2O_2$** —Translocation of cytosolic TRPC6-containing vesicles to the plasma membrane is a recently found mechanism for TRPC6 channel activation (40, 41). To determine whether the trafficking mechanism was involved in the  $H_2O_2$ -induced TRPC6 activation, we conducted biotinylation and confocal microscopy assays. In the TRPC6-expressing cells, treatment with  $H_2O_2$  at  $10 \mu M$  for 3 min remarkably and significantly increased the expression level of biotinylated TRPC6 protein ( $\sim 1$ -fold), which was not observed in the mock-transfected cells (Fig. 8, A and B). The biotinylated membrane fractions were not contaminated by non-plasma membrane proteins because the actin, a cytoskeletal protein, was negligible in the biotinylated fractions but was clearly present in the corresponding whole-cell lysates (Fig. 8A, *Inputs*). The biochemical data were corroborated by a fluorescent confocal microscopy assay. In the cells transfected with EGFP-tagged TRPC6 (at the C terminus), we were able to visualize a real time change in abundance of TRPC6 protein in the region of the plasma membrane in response to  $H_2O_2$  stimulation. Different from diffuse distribution of EGFP, the exogenous TRPC6 was primarily present in the peripheral region (the plasma membrane or

sub-plasma membrane) of the cells (Fig. 8C and [supplemental Fig. S2](#)).  $H_2O_2$  ( $10 \mu M$ ) treatment stimulated accumulation of TRPC6 proteins in the area of the plasma membrane, indicated by an apparent increase in fluorescent intensity. This response occurred within 1 min of treatment and reached the maximum at the 3rd min after  $H_2O_2$  treatment (Fig. 8C and [supplemental Fig. S2](#)). However, this effect was not observed in EGFP-transfected cells. Semiquantitative analysis revealed a significant increase (by 10–20%) in the fluorescence intensity in the plasma membrane region in a time frame of 1–5 min after application of  $H_2O_2$  in TRPC6-EGFP transfected cells, but not in EGFP alone transfected cells. To determine the physiological relevance of the ROS effect, we co-transfected HEK293 cells with TRPC6-EGFP and V1R. Next, we examined if AVP stimulated the membrane recruitment of TRPC6 and if  $H_2O_2$  contributed to the response. As shown in Fig. 8E, AVP ( $100$  nM) did not increase the fluorescence intensity in the plasma membrane of the cells transfected with EGFP and V1R, but did significantly increase the plasma membrane fluorescence in the cells trans-

## Regulation of TRPC6 by Reactive Oxygen Species

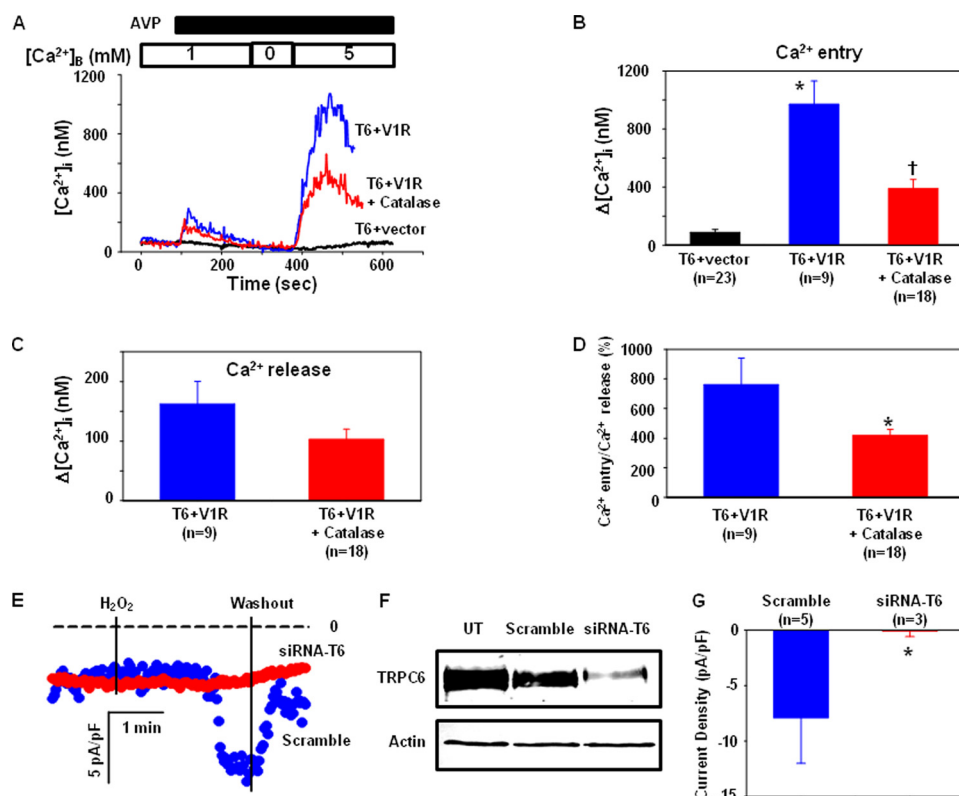


**FIGURE 4.** A–D,  $\text{Ca}^{2+}$  imaging experiments, showing involvement of endogenous  $\text{H}_2\text{O}_2$  in AVP-stimulated  $\text{Ca}^{2+}$  entry. **A**, representative traces, showing the AVP-evoked  $\text{Ca}^{2+}$  response in HEK293T cells expressing TRPC6 and an empty vector (*T6+vector*) or in cells co-transfected with TRPC6 and AVP V1R in the presence (*T6+V1R+Catalase*) or absence (*T6+V1R*) of PEG-catalase (250 units/ml for 30 min).  $\text{Ca}^{2+}$  concentration in the bathing solution is indicated by the numbers inside the top open bar. Application of 100 nM AVP is indicated by the top solid bar.  $[\text{Ca}^{2+}]_i$  indicates the  $\text{Ca}^{2+}$  concentration in the bathing solution. **B**, summary data, showing  $\text{Ca}^{2+}$  entry responses in different groups. \*,  $p < 0.05$ , compared with *T6+vector*; †,  $p < 0.05$ , compared with *T6+vector* and *T6+V1R*. **C**, effect of catalase on AVP-induced  $\text{Ca}^{2+}$  release in cells co-transfected with TRPC6 and AVP V1R. **D**, effect of catalase on normalized  $\text{Ca}^{2+}$  entry (ratio of  $\text{Ca}^{2+}$  entry to  $\text{Ca}^{2+}$  release) in response to AVP stimulation. \*,  $p < 0.05$ , compared with *T6+V1R*. **B–D**,  $n$  indicates the number of cells analyzed from 4 to 5 sets of transfection. **E–G**, in A7r5 cells. **E**, whole-cell patch clamp, showing inward currents in response to 100  $\mu\text{M}$   $\text{H}_2\text{O}_2$  in A7r5 with (*siRNA-T6*) and without (*Scramble*) knockdown of TRPC6 at a holding potential of  $-60$  mV. The dashed lines indicate zero currents. Application and removal of  $\text{H}_2\text{O}_2$  were indicated by the vertical lines. **F**, Western blot, showing TRPC6 expression levels in A7r5 cells transfected with TRPC6 siRNA sequence (*siRNA-T6*) and scrambled sequence (*Scramble*). Actin served as a loading control. **UT**, untransfected. **G**, summary data, showing the  $\text{H}_2\text{O}_2$  effect on whole-cell currents in A7r5 cells with (*siRNA-T6*) and without (*Scramble*) knockdown of TRPC6. The responses were measured by the difference between the membrane current before application of  $\text{H}_2\text{O}_2$  and the peak current after application of  $\text{H}_2\text{O}_2$ . The whole-cell currents were expressed as current density (pA/pF), normalized to the cell membrane capacitance.  $n$  indicates the number of cells analyzed from three sets of transfection. Asterisk indicates statistically significant difference compared with *Scramble* (Student's *t* test).

fected with both TRPC6-EGFP and V1R. The AVP-induced TRPC6 trafficking was significantly inhibited by pretreating the cells with PEG-catalase (250 units/ml for 30 min). These results suggest that  $\text{H}_2\text{O}_2$  triggers the translocation of TRPC6 protein to the cell surface.

## DISCUSSION

$\text{H}_2\text{O}_2$  is a small, diffusible, and ubiquitous molecule that can be synthesized and destroyed rapidly in response to external stimuli. It is well known that concentration as well as time of exposure plays an important role in the response generated by ROS (42). With respect to the concentration, it has been shown that a level above 100  $\mu\text{M}$  of  $\text{H}_2\text{O}_2$  is pathophysiologically relevant (43). A concentration of 500  $\mu\text{M}$  of  $\text{H}_2\text{O}_2$  can trigger release of  $\text{Ca}^{2+}$  from the endoplasmic reticulum and consequently activates store-operated  $\text{Ca}^{2+}$  channels (6). In this study, we used a much lower concentration of  $\text{H}_2\text{O}_2$  (10  $\mu\text{M}$ ) that showed a nearly maximal effect on TRPC6 channel activation (Fig. 2B), suggesting a physiological role of  $\text{H}_2\text{O}_2$  in TRPC6 activation.

It has been recently demonstrated that ROS can regulate the function of  $\text{Ca}^{2+}$  channels both physiologically and in diseased states (4, 5, 44). TRPC6 is a  $\text{Ca}^{2+}$ -permeable channel, activation of which is linked to a G protein-coupled receptor or receptor tyrosine kinase signaling pathway (12, 19). This signaling pathway also generates  $\text{H}_2\text{O}_2$ , which is critical for agonist-initiated signal transduction (8–11). We speculated that the widely expressed TRPC6 channel might be a target of  $\text{H}_2\text{O}_2$  in both physiological and pathological processes. Our results from two lines of experiments in this study support a physiological relevance of the redox regulation of TRPC6 channels. First,  $\text{H}_2\text{O}_2$  was generated by activation of AVP V1R, and the ROS derived from this signaling pathway contributed to TRPC6 channel activation in a heterologous expression system (Fig. 4, A–D). Second,

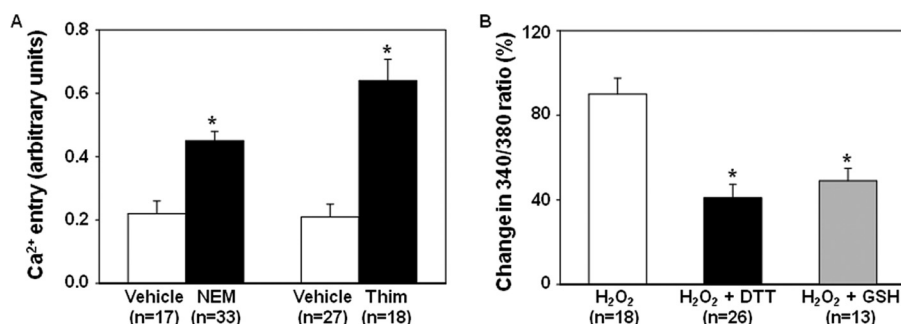


**FIGURE 5.** Effect of thiol group oxidation and reduction on TRPC6-mediated  $\text{Ca}^{2+}$  response. **A**,  $\text{Ca}^{2+}$  entry response in TRPC6-expressing cells with treatments of NEM (300  $\mu\text{M}$ ) and thimerosal (*Thim*, 100  $\mu\text{M}$ ), and their vehicles (DMSO for NEM and  $\text{H}_2\text{O}$  for thimerosal). \*,  $p < 0.05$ , compared with corresponding vehicle.  $n$  indicates the number of cells analyzed. **B**, percent increases in the intracellular  $\text{Ca}^{2+}$  levels upon  $\text{Ca}^{2+}$  readdition in TRPC6-expressing cells with the treatments of  $\text{H}_2\text{O}_2$  (10  $\mu\text{M}$ ),  $\text{H}_2\text{O}_2$  plus DTT (1 mM), or  $\text{H}_2\text{O}_2$  plus GSH-MEE (1 mM). DTT was applied  $\sim 2$  min prior to  $\text{H}_2\text{O}_2$  application. \*,  $p < 0.05$ , compared with  $\text{H}_2\text{O}_2$  group.  $n$  indicates the number of cells analyzed. Each group in **A** and **B** represents the cells from 5 to 6 sets of transfection.

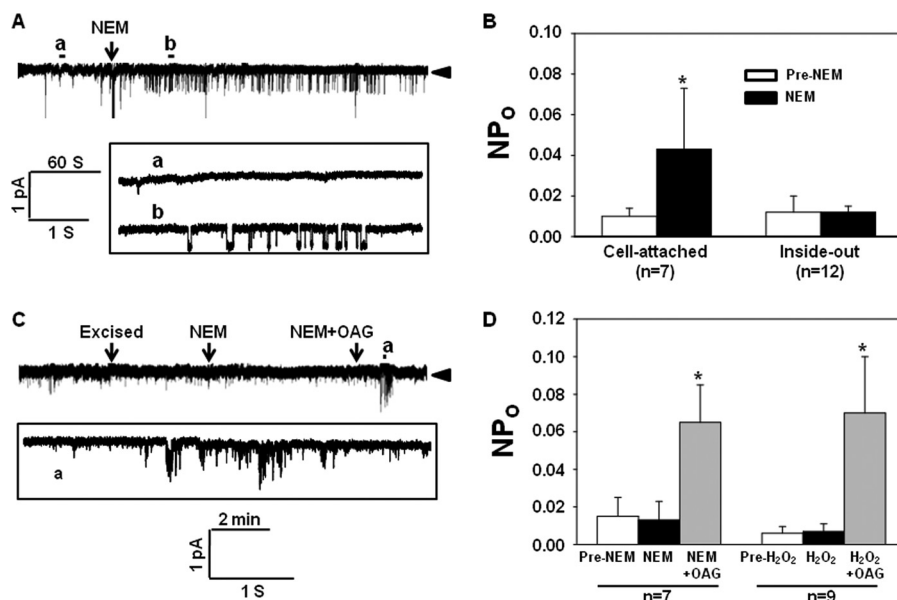


**FIGURE 6. Patch clamp experiments, analyzing the sites of thiol groups involved in TRPC6 channel activation.** All experiments were carried out in TRPC6-expressing HEK293T cells. *A*, representative traces of single channel recordings in a cell-attached patch. *Upper panel*, a real time continuous recording. *Arrowhead*, the closed state of channels. *Bottom panel*, the time-expanded portions of the selected regions in the *upper trace*. *B*, summary data, showing the effect of NEM (300  $\mu$ M) on  $NP_0$  of TRPC6 channels in the cell-attached and inside-out mode of patch clamp recordings. \*,  $p < 0.05$ , compared with pre-NEM (paired Student's *t* test). *n* indicates the number of analyzed cells with four to five sets of transfection. *C*, representative traces in an inside-out patch recording, showing the channel activity before and after application of NEM and NEM+OAG. *Arrowhead*, the closed state of channels. The *bottom trace* is a time-expanded portion of the region in the *upper trace*, as indicated. *D*, summary data, showing the effect of NEM, H<sub>2</sub>O<sub>2</sub>, and OAG on TRPC6 channel activity in the inside-out patch clamp mode. Asterisk indicates  $p < 0.05$ , compared with other groups (one-way repeated measures analysis of variance). *n* indicates the number of analyzed cells with four sets of transfection.

endogenous TRPC6 in vascular smooth muscle cells fully contributed to H<sub>2</sub>O<sub>2</sub>-stimulated membrane currents (Fig. 4, *E* and *F*). The importance of these findings is that, physiologically, full activation of TRPC6 channel by an agonist may require a certain level of intracellular H<sub>2</sub>O<sub>2</sub>. Thus, it is conceivable that overproduction of ROS in disease states may cause hyperactivity of the TRPC6 channel. Indeed, the currently known TRPC6-related disorders or diseases are associated with overproduction of ROS (1, 4, 19, 23–25, 45, 46).

Several members of the TRP superfamily have been demonstrated to be redox-sensitive. These include TRPA1, TRPM2, TRPC3, TRPC4, and TRPC5 (6, 26, 27, 47–49). In a recent study by Yoshida *et al.* (26), TRPC5 was reported to be a channel that elicited a robust Ca<sup>2+</sup> response to H<sub>2</sub>O<sub>2</sub>, although the TRPC6 response was relatively weak. We did not compare the H<sub>2</sub>O<sub>2</sub>-induced Ca<sup>2+</sup> response between TRPC5- and TRPC6-expressing cells in this study. However, our data suggest that H<sub>2</sub>O<sub>2</sub> itself did significantly activate TRPC6 channel at a concentration of 10  $\mu$ M. Several potential possibilities could contribute to the discrepancy between their study and ours. These include potentially different expression levels of TRPC6 protein in human embryonic kidney cells, different experimental protocols (Ca<sup>2+</sup> readmission in our study *versus* continuous Ca<sup>2+</sup> existence in their study), and different extracellular Ca<sup>2+</sup> concentrations (5 mM in ours *versus* 2 mM in theirs). Other differences might also exist between our system and theirs, some of which include a difference in the passage of HEK293T cells as well as differences in the level and activity of endogenous intracellular antioxidants or ROS-decomposing enzymes.

There are two fundamental questions concerning the mechanisms underlying the H<sub>2</sub>O<sub>2</sub> effect on TRPC6 channels. First, what is the target molecule of H<sub>2</sub>O<sub>2</sub> in this signaling pathway? ROS are believed to inter-

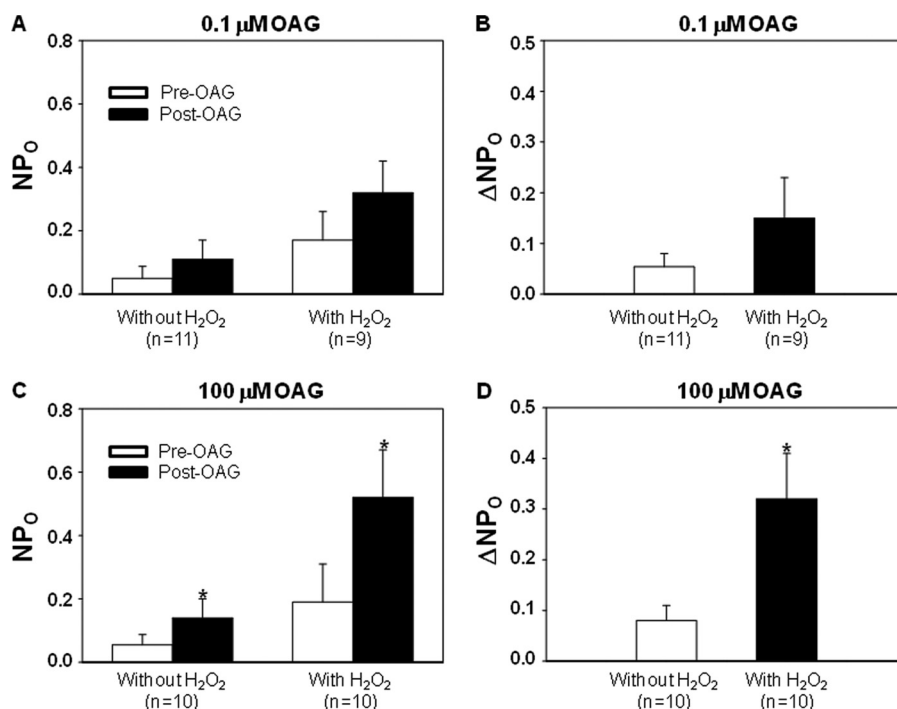


**FIGURE 7. Cell-attached patch clamp, showing the OAG effect on channel activity in TRPC6 expressing HEK293T cells with and without pretreatment with H<sub>2</sub>O<sub>2</sub> (10  $\mu$ M for 3 min).** *A* and *B*, cells were stimulated with 0.1  $\mu$ M OAG. *C* and *D*, cells were stimulated with 100  $\mu$ M OAG. *A* and *C* indicate the channel activity ( $NP_0$ ) before and after OAG treatment in the presence and absence of H<sub>2</sub>O<sub>2</sub>. *B* and *D* show the difference in OAG-induced increase in channel activity ( $\Delta NP_0$ ) with and without existence of H<sub>2</sub>O<sub>2</sub>. *n* indicates the number of cells analyzed, and each group represents at least four sets of transfection. \*,  $p < 0.05$ , *versus* pre-OAG in *C*, and *versus* "Without H<sub>2</sub>O<sub>2</sub>" in *D*.

## Regulation of TRPC6 by Reactive Oxygen Species

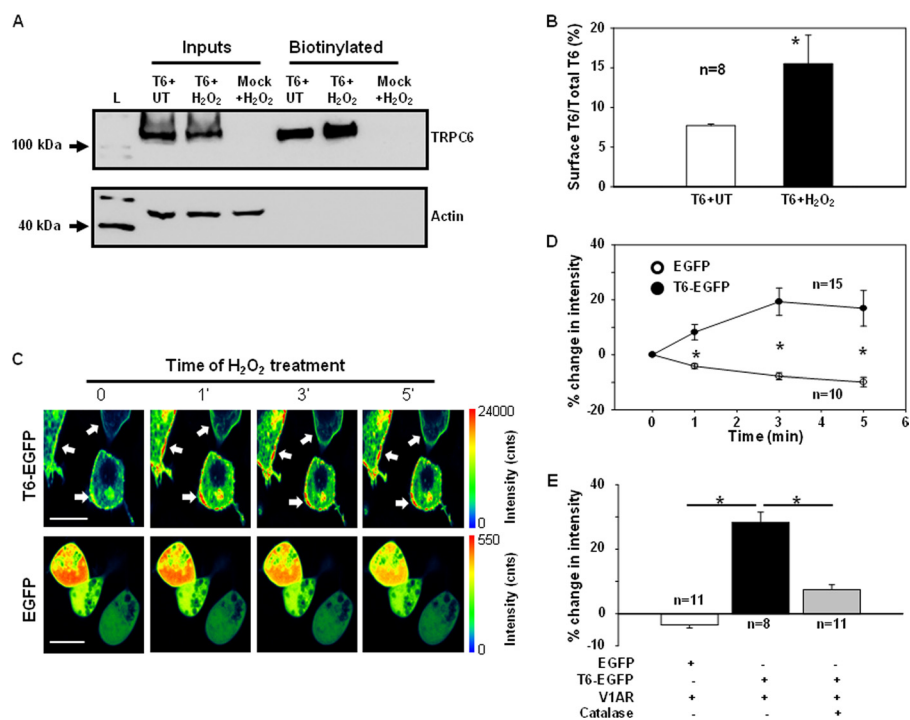


**FIGURE 8. Analysis of TRPC6 trafficking to the cell surface in response to H<sub>2</sub>O<sub>2</sub>.** *A*, biotinylation of TRPC6 protein in HEK293T cells transfected with TRPC6 (*T6*) or empty vector (*Mock*) with and without H<sub>2</sub>O<sub>2</sub> stimulation. *L*, a protein ladder; *T6+UT*, TRPC6-expressing cells without H<sub>2</sub>O<sub>2</sub> treatment; *T6+H<sub>2</sub>O<sub>2</sub>*, TRPC6-expressing cells treated with 10 μM H<sub>2</sub>O<sub>2</sub> for 3 min; *Mock+H<sub>2</sub>O<sub>2</sub>*, empty vector-transfected cells treated with 10 μM H<sub>2</sub>O<sub>2</sub> for 3 min; *Inputs*, the whole-cell lysates (unbiotinylated), ~1:10 of the lysates used for biotinylation. *B*, quantitative analysis of the cell surface TRPC6 protein with and without H<sub>2</sub>O<sub>2</sub> stimulation. Data were expressed as percentages of integrated optical density of TRPC6 immunoblots in biotinylated fractions to the corresponding inputs, calculated by (integrated optical density of biotinylated TRPC6 blot / (integrated optical density of TRPC6 blot in input × 10)) × 100. *n* indicates the number of independent experiments. The optical density of immunoblots was measured with a software provided by AlphaEaseFC Imaging System (Alpha Innotech). *Asterisk* indicates significant difference compared with *T6+UT*. *C*, representative confocal microscopy photographs, showing TRPC6 trafficking to the region of the plasma membrane in response to 10 μM H<sub>2</sub>O<sub>2</sub> stimulation in the cells transfected with TRPC6-EGFP (*T6-EGFP*), but not in the cells transfected with EGFP alone. Images were consecutively captured before application, immediately, 2, and 4 min after application of H<sub>2</sub>O<sub>2</sub> (labeled with 0, 1', 3', and 5', respectively). The duration of scanning one image was ~1 min. The *rainbow bars* on the right indicates the fluorescence intensity in arbitrary units. *Arrows* indicate the sites of an increase in fluorescence intensity compared with before application of H<sub>2</sub>O<sub>2</sub> (*time 0*). The *horizontal bars* in the *left panels* represent 20 μm. *D*, time course changes in fluorescence intensity on the cell surface in response to H<sub>2</sub>O<sub>2</sub> in TRPC6-EGFP (*T6-EGFP*) or EGFP alone (*EGFP*) transfected cells. Data were expressed as percent changes from the values before application of H<sub>2</sub>O<sub>2</sub> (*time 0*). The fluorescence intensity was measured using the software SymPhoTime (version 5.0). *Asterisk* indicates significant difference between *T6-EGFP* and *EGFP* at the corresponding time point. *n* indicates the number of analyzed cells from four sets of transfection. *E*, percent changes in fluorescence intensity on the cell surface 3 min after application of AVP (100 nM) in HEK293 cells cotransfected with EGFP or TRPC6-EGFP (*T6-EGFP*) and V1R with and without pretreatment of PEG-catalase (250 units/ml for 30 min). See *D* for the approach for data analysis. *Asterisk* indicates significant difference between the indicated groups. *n* indicates the number of analyzed cells from four sets of transfection.

act with cell signaling pathways by way of modification of key thiol groups on proteins (44). The results from this study suggest that this is also the case in the H<sub>2</sub>O<sub>2</sub>-dependent TRPC6 activation. NEM and thimerosal, both of which are thiol-specific oxidizing agents (50, 51), were able to mimic the H<sub>2</sub>O<sub>2</sub> response. Conversely, DTT and GSH-MEE, both of which are thiol-specific reducing agents (50, 51), antagonized the H<sub>2</sub>O<sub>2</sub> effect on TRPC6 (Fig. 5).

The next question is where the thiol group-containing proteins are located. H<sub>2</sub>O<sub>2</sub> could oxidize the cysteine residues present in the TRPC6 protein directly or oxidize the thiol groups in other proteins that regulate the TRPC6 channels. Recently, it has been reported that the redox-sensitive cysteine residues were implicated in modulation of transient receptor potential channel function (26, 52). Among the 931

amino acids of full-length human TRPC6, there are 15 cysteines that are localized either in the N terminus or in the transmembrane segments. We originally speculated that one or more specific cysteine residues in the sequence might confer TRPC6 channel redox sensitivity. To our surprise, our data did not support the mechanism of direct oxidation of the TRPC6 protein because H<sub>2</sub>O<sub>2</sub><sup>-</sup> or NEM-induced TRPC6 channel activation was only observed in the whole-cell and/or cell-attached patches (Fig. 3 and Fig. 6, *A* and *B*). However, in the inside-out excised patches where TRPC6 channel is fully accessible, yet cell integrity and physiological milieu are disrupted, both NEM and H<sub>2</sub>O<sub>2</sub> failed to activate the channel (Fig. 6, *B–D*). Taken together, these data strongly suggest that activation of TRPC6 channel by H<sub>2</sub>O<sub>2</sub> is not through direct oxidation of the TRPC6 protein itself but via an indirect mechanism that requires cytosolic component(s). The potential candidate of the intracellular mediator(s) could be protein-tyrosine kinases or protein-tyrosine phosphatases. It has been reported that oxidative activation of *Src* is a downstream mechanism in H<sub>2</sub>O<sub>2</sub>-dependent cellular responses (53–55). In particular, protein-tyrosine phosphatases have been known to be important protein targets of H<sub>2</sub>O<sub>2</sub> because all the phosphatases contain an essential cysteine residue with low p*K<sub>a</sub>* (4.7–5.4), which is vulnerable to oxidation by H<sub>2</sub>O<sub>2</sub> (2, 56, 57). Oxidative inactivation of spe-

cific protein-tyrosine phosphatases, such as protein-tyrosine phosphatases 1B, SHP-1, and SHP-2, has been described as a downstream mechanism in H<sub>2</sub>O<sub>2</sub>-dependent cellular responses (2, 7, 58, 59). Thus, it is very likely that H<sub>2</sub>O<sub>2</sub> would regulate the activity of the redox-sensitive kinases and/or phosphatases to alter the phosphorylation status of the TRPC6 channel, which leads to the activation of TRPC6 channels. In support of this notion, a recent study demonstrated that the activity of TRPC6 channel was regulated by tyrosine phosphorylation in response to epidermal growth factor stimulation (60).

Multiple mechanisms could be involved in H<sub>2</sub>O<sub>2</sub>-induced TRPC6 channel activation. DAG is generated from the phospholipase C signaling pathway and is a widely accepted physiological activator of the TRPC6 channel (34). Our data suggest that H<sub>2</sub>O<sub>2</sub> can enhance the sensitivity of TRPC6 channel

to DAG. Because  $H_2O_2$  is also generated from the phospholipase C signaling pathway, this study provides a novel view that ligand binding-associated TRPC6 activation involves both DAG and  $H_2O_2$ . The synergistic effect of the two molecules ensures a full and accelerated activation of the channel after initiation of the phospholipase C signaling cascade. Recently, a synergistic activation of TRPC6 channel by receptor and mechanical stimulation was reported in vascular smooth muscle cells (61).

TRPC6 channel trafficking to the plasma membrane is another mechanism for activation in response to agonist stimulation (40, 41). Interestingly, we found that  $H_2O_2$  treatment clearly stimulated the membrane recruitment of TRPC6 protein (Fig. 8), suggesting that promotion of TRPC6 channel translocation to the cell surface is one potential mechanism for  $H_2O_2$ -induced TRPC6 currents and  $Ca^{2+}$  response. Insertion of new channels to the plasma membrane usually leads to simultaneous opening of multiple channels in a cell-attached patch. This phenomenon was not clearly observed in our recordings. It could be explained by a relatively low  $NP_o$  of the channel and a small percentage (~20%) of the channel protein recruited to the cell surface in response to  $H_2O_2$ . We currently do not know the mechanism underlying the  $H_2O_2$ -stimulated TRPC6 protein trafficking. It may involve several redox-sensitive protein kinases or protein-tyrosine phosphatases that alter the phosphorylation state of trafficking-related proteins. Further mechanistic studies are required to fully delineate the entire signaling cascade.

Recently, regulation of TRPC channels by membrane lipids has drawn intense attention (62–64). For instance, phosphatidylinositol 4,5-bisphosphate has been reported to directly activate exogenous TRPC3, -6, and -7 in human embryonic kidney cells (63) but to inhibit native TRPC6 channels in isolated mesenteric artery myocytes (62). Phosphatidylinositol 3,4,5-trisphosphate promotes TRPC6 activity by binding the calmodulin-binding site in the TRPC6 C terminus (64). Thus, another potential mechanism for the  $H_2O_2$  effect is to modulate the interaction between phospholipids and TRPC6 through oxidation of these membrane-delimited lipids or the enzymes that metabolize the lipids. However, both  $H_2O_2$  and NEM activated TRPC6 channel only in the cell-attached mode but not in the excised mode of patch recordings. These results strongly suggest that oxidation of the membrane lipids or the membrane-localized enzymes that metabolize the lipids might not be involved in the  $H_2O_2$ -induced TRPC6 activation.

In summary, this study provided evidence that  $H_2O_2$  is an activator of TRPC6 channel. This  $H_2O_2$ -dependent channel response is through modification of thiol groups in one or more of the intracellular redox-sensitive proteins. Oxidation of the intermediators in turn activates the TRPC6 channel, sensitizes the channel to other physiological stimuli like DAG, and promotes TRPC6 channel trafficking to the plasma membrane. Given that  $H_2O_2$  is a ubiquitous molecule whose generation is involved in both physiological and pathological processes (4, 44, 45) and that TRPC6 is a widely expressed channel that is involved in both health and disease, the novel regulatory mechanism of TRPC6 channel by  $H_2O_2$  may have important physiological and clinical relevance.

*Acknowledgment*—We thank Dr. Davis Saffen (Department of Pharmacology, Ohio State University, Columbus, OH) for providing us with pEF-BOS-SK-TRPC6A constructs.

## REFERENCES

- Lassègue, B., and Griendling, K. K. (2004) *Am. J. Hypertens.* **17**, 852–860
- Rhee, S. G., Chang, T. S., Bae, Y. S., Lee, S. R., and Kang, S. W. (2003) *J. Am. Soc. Nephrol.* **14**, S211–S215
- Gianni, D., Bohl, B., Courtneidge, S. A., and Bokoch, G. M. (2008) *Mol. Biol. Cell* **19**, 2984–2994
- Hidalgo, C., and Donoso, P. (2008) *Antioxid. Redox. Signal.* **10**, 1275–1312
- Schnackenberg, C. G. (2002) *Curr. Opin. Pharmacol.* **2**, 121–125
- Hecquet, C. M., Ahmmed, G. U., Vogel, S. M., and Malik, A. B. (2008) *Circ. Res.* **102**, 347–355
- Weibrecht, I., Böhmer, S. A., Dagnell, M., Kappert, K., Ostman, A., and Böhmer, F. D. (2007) *Free Radic. Biol. Med.* **43**, 100–110
- Block, K., Eid, A., Griendling, K. K., Lee, D. Y., Wittrant, Y., and Gorin, Y. (2008) *J. Biol. Chem.* **283**, 24061–24076
- Zafari, A. M., Ushio-Fukai, M., Akers, M., Yin, Q., Shah, A., Harrison, D. G., Taylor, W. R., and Griendling, K. K. (1998) *Hypertension* **32**, 488–495
- Sundaresan, M., Yu, Z. X., Ferrans, V. J., Irani, K., and Finkel, T. (1995) *Science* **270**, 296–299
- Bae, Y. S., Kang, S. W., Seo, M. S., Baines, I. C., Tekle, E., Chock, P. B., and Rhee, S. G. (1997) *J. Biol. Chem.* **272**, 217–221
- Venkatachalam, K., and Montell, C. (2007) *Annu. Rev. Biochem.* **76**, 387–417
- Pedersen, S. F., Owsianik, G., and Nilius, B. (2005) *Cell Calcium* **38**, 233–252
- Ramsey, I. S., Delling, M., and Clapham, D. E. (2006) *Annu. Rev. Physiol.* **68**, 619–647
- Cayouette, S., and Boulay, G. (2007) *Cell Calcium* **42**, 225–232
- Dietrich, A., Kalwa, H., Fuchs, B., Grimminger, F., Weissmann, N., and Gudermann, T. (2007) *Cell Calcium* **42**, 233–244
- Zhou, J., Du, W., Zhou, K., Tai, Y., Yao, H., Jia, Y., Ding, Y., and Wang, Y. (2008) *Nat. Neurosci.* **11**, 741–743
- Onohara, N., Nishida, M., Inoue, R., Kobayashi, H., Sumimoto, H., Sato, Y., Mori, Y., Nagao, T., and Kurose, H. (2006) *EMBO J.* **25**, 5305–5316
- Dietrich, A., and Gudermann, T. (2007) *Handb. Exp. Pharmacol.* **179**, 125–141
- Inoue, R., Okada, T., Onoue, H., Hara, Y., Shimizu, S., Naitoh, S., Ito, Y., and Mori, Y. (2001) *Circ. Res.* **88**, 325–332
- Sours, S., Du, J., Chu, S., Ding, M., Zhou, X. J., and Ma, R. (2006) *Am. J. Physiol. Renal Physiol.* **290**, F1507–F1515
- Reiser, J., Polu, K. R., Möller, C. C., Kenlan, P., Altintas, M. M., Wei, C., Faul, C., Herbert, S., Villegas, I., Avila-Casado, C., McGee, M., Sugimoto, H., Brown, D., Kalluri, R., Mundel, P., Smith, P. L., Clapham, D. E., and Pollak, M. R. (2005) *Nat. Genet.* **37**, 739–744
- Möller, C. C., Wei, C., Altintas, M. M., Li, J., Greka, A., Ohse, T., Pippin, J. W., Rastaldi, M. P., Wawersik, S., Schiavi, S., Henger, A., Kretzler, M., Shankland, S. J., and Reiser, J. (2007) *J. Am. Soc. Nephrol.* **18**, 29–36
- Winn, M. P., Daskalakis, N., Spurney, R. F., and Middleton, J. P. (2006) *J. Am. Soc. Nephrol.* **17**, 378–387
- Watanabe, H., Murakami, M., Ohba, T., Takahashi, Y., and Ito, H. (2008) *Pharmacol. Ther.* **118**, 337–351
- Yoshida, T., Inoue, R., Morii, T., Takahashi, N., Yamamoto, S., Hara, Y., Tominaga, M., Shimizu, S., Sato, Y., and Mori, Y. (2006) *Nat. Chem. Biol.* **2**, 596–607
- Hara, Y., Wakamori, M., Ishii, M., Maeno, E., Nishida, M., Yoshida, T., Yamada, H., Shimizu, S., Mori, E., Kudoh, J., Shimizu, N., Kurose, H., Okada, Y., Imoto, K., and Mori, Y. (2002) *Mol. Cell* **9**, 163–173
- Du, J., Sours-Brothers, S., Coleman, R., Ding, M., Graham, S., Kong, D. H., and Ma, R. (2007) *J. Am. Soc. Nephrol.* **18**, 1437–1445
- Graham, S., Ding, M., Sours-Brothers, S., Yorio, T., Ma, J. X., and Ma, R. (2007) *Am. J. Physiol. Renal Physiol.* **293**, F1381–F1390
- Ma, R., Rundle, D., Jacks, J., Koch, M., Downs, T., and Tsiokas, L. (2003)

## Regulation of TRPC6 by Reactive Oxygen Species

- J. Biol. Chem.* **278**, 52763–52772
31. Ma, R., Li, W. P., Rundle, D., Kong, J., Akbarali, H. I., and Tsiokas, L. (2005) *Mol. Cell. Biol.* **25**, 8285–8298
32. Du, J., Ding, M., Sours-Brothers, S., Graham, S., and Ma, R. (2008) *Am. J. Physiol. Renal Physiol.* **294**, F909–F918
33. Gryniewicz, G., Poenie, M., and Tsien, R. Y. (1985) *J. Biol. Chem.* **260**, 3440–3450
34. Hofmann, T., Obukhov, A. G., Schaefer, M., Harteneck, C., Gudermann, T., and Schultz, G. (1999) *Nature* **397**, 259–263
35. Soboloff, J., Spassova, M., Xu, W., He, L. P., Cuesta, N., and Gill, D. L. (2005) *J. Biol. Chem.* **280**, 39786–39794
36. Tsvilovskyy, V. V., Zholos, A. V., Aberle, T., Philipp, S. E., Dietrich, A., Zhu, M. X., Birnbaumer, L., Freichel, M., and Flockerzi, V. (2009) *Gastroenterology* **137**, 1415–1424
37. Nishida, M., Watanabe, K., Sato, Y., Nakaya, M., Kitajima, N., Ide, T., Inoue, R., and Kurose, H. (2010) *J. Biol. Chem.* **285**, 13244–13253
38. Yu, Y., Keller, S. H., Remillard, C. V., Safrina, O., Nicholson, A., Zhang, S. L., Jiang, W., Vangala, N., Landsberg, J. W., Wang, J. Y., Thistlethwaite, P. A., Channick, R. N., Robbins, I. M., Loyd, J. E., Ghofrani, H. A., Grimminger, F., Schermuly, R. T., Cahalan, M. D., Rubin, L. J., and Yuan, J. X. (2009) *Circulation* **119**, 2313–2322
39. Dietrich, A., Mederos, y., Schnitzler, M., Emmel, J., Kalwa, H., Hofmann, T., and Gudermann, T. (2003) *J. Biol. Chem.* **278**, 47842–47852
40. Chaudhuri, P., Colles, S. M., Bhat, M., Van Wagoner, D. R., Birnbaumer, L., and Graham, L. M. (2008) *Mol. Biol. Cell* **19**, 3203–3211
41. Cayouette, S., Lussier, M. P., Mathieu, E. L., Bousquet, S. M., and Boulay, G. (2004) *J. Biol. Chem.* **279**, 7241–7246
42. Schröder, E., and Eaton, P. (2008) *Curr. Opin. Pharmacol.* **8**, 153–159
43. Ward, P. A. (1991) *Am. J. Med.* **91**, 89S–94S
44. Hool, L. C., and Corry, B. (2007) *Antioxid. Redox. Signal.* **9**, 409–435
45. Cave, A. C., Brewer, A. C., Narayanapanicker, A., Ray, R., Grieve, D. J., Walker, S., and Shah, A. M. (2006) *Antioxid. Redox. Signal.* **8**, 691–728
46. Wilcox, C. S. (2002) *Curr. Hypertens. Rep.* **4**, 160–166
47. Andersson, D. A., Gentry, C., Moss, S., and Bevan, S. (2008) *J. Neurosci.* **28**, 2485–2494
48. Poteser, M., Graziani, A., Rosker, C., Eder, P., Derler, I., Kahr, H., Zhu, M. X., Romanin, C., and Groschner, K. (2006) *J. Biol. Chem.* **281**, 13588–13595
49. Xu, S. Z., Sukumar, P., Zeng, F., Li, J., Jairaman, A., English, A., Naylor, J., Ciurtin, C., Majeed, Y., Milligan, C. J., Bahnasi, Y. M., Al-Shawaf, E., Porter, K. E., Jiang, L. H., Emery, P., Sivaprasadarao, A., and Beech, D. J. (2008) *Nature* **451**, 69–72
50. Hsu, M. F., Sun, S. P., Chen, Y. S., Tsai, C. R., Huang, L. J., Tsao, L. T., Kuo, S. C., and Wang, J. P. (2005) *Biochem. Pharmacol.* **70**, 1320–1329
51. Edwards, D. H., Li, Y., and Griffith, T. M. (2008) *Arterioscler. Thromb. Vasc. Biol.* **28**, 1774–1781
52. Macpherson, L. J., Dubin, A. E., Evans, M. J., Marr, F., Schultz, P. G., Cravatt, B. F., and Patapoutian, A. (2007) *Nature* **445**, 541–545
53. Chen, K., Vita, J. A., Berk, B. C., and Keaney, J. F., Jr. (2001) *J. Biol. Chem.* **276**, 16045–16050
54. Gervásio, O. L., Whitehead, N. P., Yeung, E. W., Phillips, W. D., and Allen, D. G. (2008) *J. Cell Sci.* **121**, 2246–2255
55. Suzuki, Y., Yoshizumi, M., Kagami, S., Koyama, A. H., Taketani, Y., Houchi, H., Tsuchiya, K., Takeda, E., and Tamaki, T. (2002) *J. Biol. Chem.* **277**, 9614–9621
56. Denu, J. M., and Dixon, J. E. (1998) *Curr. Opin. Chem. Biol.* **2**, 633–641
57. Soulsby, M., and Bennett, A. M. (2009) *Physiology* **24**, 281–289
58. Tabet, F., Schiffrin, E. L., Callera, G. E., He, Y., Yao, G., Ostman, A., Kappert, K., Tonks, N. K., and Touyz, R. M. (2008) *Circ. Res.* **103**, 149–158
59. Lou, Y. W., Chen, Y. Y., Hsu, S. F., Chen, R. K., Lee, C. L., Khoo, K. H., Tonks, N. K., and Meng, T. C. (2008) *FEBS J.* **275**, 69–88
60. Hisatsune, C., Kuroda, Y., Nakamura, K., Inoue, T., Nakamura, T., Michikawa, T., Mizutani, A., and Mikoshiba, K. (2004) *J. Biol. Chem.* **279**, 18887–18894
61. Inoue, R., Jensen, L. J., Jian, Z., Shi, J., Hai, L., Lurie, A. I., Henriksen, F. H., Salomonsson, M., Morita, H., Kawarabayashi, Y., Mori, M., Mori, Y., and Ito, Y. (2009) *Circ. Res.* **104**, 1399–1409
62. Albert, A. P., Saleh, S. N., and Large, W. A. (2008) *J. Physiol.* **586**, 3087–3095
63. Lemmonier, L., Trebak, M., and Putney, J. W., Jr. (2008) *Cell Calcium* **43**, 506–514
64. Kwon, Y., Hofmann, T., and Montell, C. (2007) *Mol. Cell* **25**, 491–503